Computational and Theoretical Analysis of Actin Polymerization

Tae Yoon Kim

Department of Mechanical Engineering, Massachusetts Institute of Technology, 77 Massachusetts Avenue, Cambridge, MA 02139

Polymerization of actin filaments is investigated via both a computational model and a continuum approach. The overall length distribution of actin filaments acquired using the computational simulation is analogous to normal distribution with its average inversely proportional to a nucleation rate. Also, the average corresponds well to theoretical prediction obtained by the continuum approach. The computational model has the potential to be applied to study the effects of numerous actin binding proteins and other factors on actin polymerization processes.

Eukaryotic cells have cytoskeleton that is a dynamic structure associated with intracellular transport and the shapes, motility, and division of cells. Actin is one of the most abundant constituents of the cytoskeleton in eukaryotic cells, and it plays a central role in numerous biological processes including migration and stability [1]. Monomeric actin (G-actin) self-assembles into filamentous actin (F-actin), governed by nucleation, elongation, and depolymerization [2]. The nucleation process is a rate-limiting step, followed by quick elongation largely at the barbed end of filaments and by depolymerization mostly at the pointed end. In addition, the filaments can be crosslinked together via various actin binding proteins, resulting in the formation of homogeneous networks or thick bundle. Due to its importance, the polymerization process of actin filaments has extensively been investigated using computational [3] and experimental studies [4]. Nevertheless, to date, a systematic approach which incorporates diverse methodologies has lacked.

This study was performed in order to comprehend the polymerization mechanism of actin filaments using a 3D computational model and a continuum approach and to compare the results from the two dissimilar methods. First, the computational model was validated in two aspects, and the length distribution of actin filaments was probed with different nucleation and elongation rates using the model. The distribution was then compared to that estimated by the continuum approach, showing a nice agreement between the two results.

A computational model is developed based on Brownian dynamics using C language. Among several approaches for Brownian dynamics, Langevin equation is employed:

$$m\mathbf{a} = \mathbf{F} - \zeta\mathbf{v} + \mathbf{F}_\mathrm{B} \tag{1}$$

where m is mass, ζ is friction coefficient, $\mathbf{v}$ is veclocity, and $\mathbf{a}$ is acceleration. $\mathbf{F}$ is a deterministic force including bending and spring, and $\mathbf{F}_\mathrm{B}$ is thermal force with zero mean. The friction coefficient can be expressed via Stokes drag, $\zeta = 3\pi\eta d$, where d is the diameter of a monomer (7 nm), and η is the viscosity of medium. The correlation of $\mathbf{F}_\mathrm{B}$ satisfies the relation of $< \mathbf{F}_{\mathrm{B},i} \cdot \mathbf{F}_{\mathrm{B},j} >= 2k_\mathrm{B}T\zeta\delta_{ij}/\Delta t$ [5], where δ_{ij} is the delta function, and Δt is a time step. Through scaling analysis, the acceleration term can be neglected, leading to the following simplified equation:

$$\mathbf{v} = \frac{\mathrm{d}\mathbf{r}}{\mathrm{d}t} = \frac{1}{\zeta}\left(\mathbf{F} + \mathbf{F}_\mathrm{B}\right) \tag{2}$$

The position of each particle is updated according to the Euler forward integration scheme:

$$\mathbf{r}(t+\Delta t) \simeq \mathbf{r}(t) + \left(\frac{\mathrm{d}\mathbf{r}}{\mathrm{d}t}\right)\Delta t \tag{3}$$

Three kinds of potentials are implemented to characterize the force behaviors of actin monomers and filaments: spring (Eq. 4), bending (Eq. 5), and Lennard-Jones repulsive forces (Eq. 6) [6]:

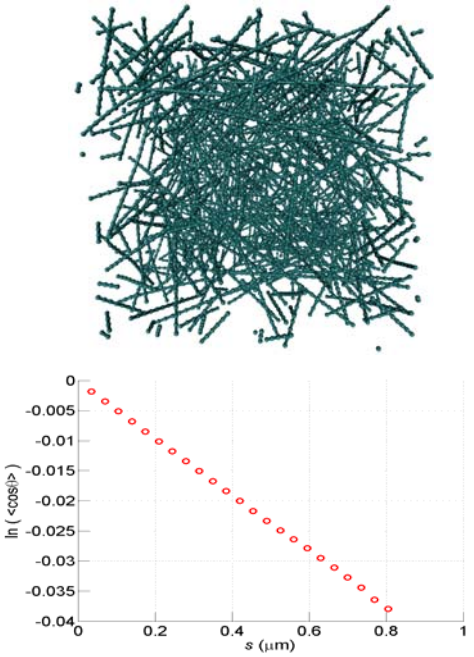

FIG. 1. (a) An example of filaments polymerized in a cubical computational domain whose width is 280 nm. Each filament is mostly straight due to large bending rigidity and has different length. (b) Average correlation function of a single filament which is 0.9 μm in length. The slope of the curve is -0.047, yielding $l_\mathrm{p} = 21.28$ μm.

$$U_s(r) = \kappa_s (r-d)^2 / 2 \quad (4)$$

$$U_b(\theta) = \kappa_b \theta^2 / 2 \quad (5)$$

$$U_r(r) = 4\varepsilon\left[(d/r)^{12} - (d/r)^6\right] \text{ when } r \le 2^{1/6} d \quad (6)$$

where ε is characteristic energy (= $k_B T$ in this model), r is distance between particles, and θ is bending angle formed by three consecutive particles on a filament. In addition, κ_s and κ_b are extensional and bending stiffness, respectively, and they are reasonably set based on values measured in experiments [7,8] (κ_s = 0.1691 N / m and κ_b = 1.243×10^{-17} N m).

The overall simulation procedure is like the following. First, in a cubical computational domain whose width is 280 nm with periodic boundary condition, 8,000 actin monomers are uniformly allocated, resulting in the actin concentration of 1.2 mM. Then, the monomers begin to thermally fluctuate in the domain according to Langevin equation. If two actin monomers are located proximately enough, they may form a stable nucleus with a small probability, P_n, and during the nucleation procedure, the directionality of the filament (barbed and pointed ends) is randomly determined. In contrast to the slow nucleation process limited by the small P_n, the elongation of filaments can instantly occur once a free monomer is positioned near the front of a barbed end of a filament, meaning that the monomer should be located near the axis of the filament. The nucleation and elongation rates are empirically found:

$$k_n = 2.5\times10^{13} \times P_n \ (\mathrm{M^{-1}s^{-1}}) \quad (7)$$

$$k_e = 1.4\times10^{9} \ (\mathrm{M^{-1}s^{-1}}) \quad (8)$$

In this model, depolymerization of filaments is neglected for simplicity. The simulation is terminated when all monomers are converted into filaments, and then the length distribution of actin filaments is measured.

The length distribution can also be estimated via a continuum approach similar to that in [9]. The number of free actin monomers (N_m) and filaments (N_f) can be expressed as:

$$\frac{dN_m}{dt} = -k_n N_m^{\,2} - k_e N_m N_f \quad (9)$$
$$\frac{dN_f}{dt} = \frac{1}{2} k_n N_m^{\,2}$$

By combining the two, a single equation is obtained:

$$\frac{\dot{N}_m}{N_m} + \frac{Z\dot{Z}}{Z(Z-1)+\beta/2} = 0 \quad (10)$$

where $\beta = k_n / k_e$, and $Z \equiv 1 + \beta(N_f / N_m)$. After the subsequent mathematical derivations, the average filament length is expressed as:

$$\langle L_f / d \rangle = \frac{N_{m,0}}{N_f} = \sqrt{\beta}\exp\left[-\frac{\arctan\left(\frac{1}{\sqrt{2\beta-1}}\right)}{\sqrt{2\beta-1}}\right] \times \frac{\sqrt{2Z^2-2Z+\beta}}{Z-1}\exp\left[\frac{\arctan\left(\frac{2Z-1}{\sqrt{2\beta-1}}\right)}{\sqrt{2\beta-1}}\right] \quad (11)$$

where $N_{m,0}$ is the initial number of free monomers. In the limit of $Z \to \infty$, the equation is simplified as:

$$\langle L_f / \sigma_A \rangle = \sqrt{2\beta}\exp\left[\frac{\pi - 2\arctan\left(\frac{1}{\sqrt{2\beta-1}}\right)}{2\sqrt{2\beta-1}}\right] \quad (12)$$

Fig. 1(a) shows a sample of polymerized filaments with P_n=10^{-7} corresponding to k_n=2.5×10^6 $\mathrm{M^{-1}s^{-1}}$. Each filament has dissimilar length and a straight shape due to the imposed large bending stiffness, κ_b. While the seeming features of actin filaments tend be realistic, additional quantitative validations are required to confirm that the model itself is rigorous. Therefore, in order to check that actin filaments behave as semiflexible polymer with correct persistence length, l_p, the average correlation function of filament orientation was estimated. [8]:

$$\langle \vec{t}(s)\cdot\vec{t}(0)\rangle = \langle \cos(\theta(s)-\theta(0))\rangle = e^{-|s|/l_p} \quad (13)$$

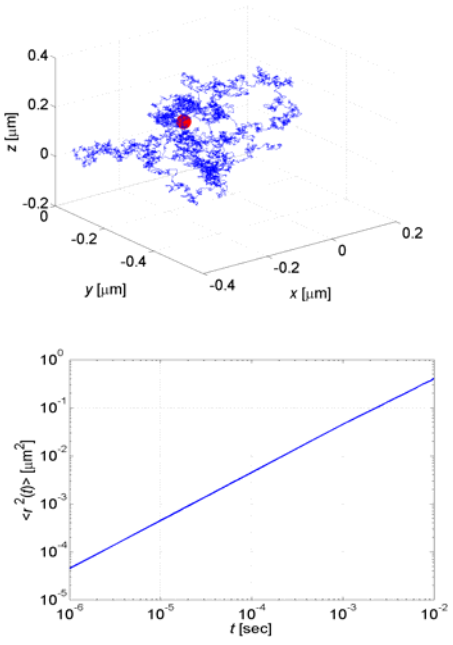

FIG. 2. (a) An example of thermal fluctuation of a free actin monomer for 0.01 sec. The red dot represents a starting point of the fluctuation at t=0 (0, 0, 0). (b) A smooth MSD curve obtained from the ensemble of thermal trajectory of many monomers.

where s is a contour coordinate, and $\vec{t}$ is a tangential unit vector. By averaging data acquired from separate simulations where a single long filament undulated for a long time, the curve in Fig. 1(b) was obtained, having the slope of -0.047 that corresponds to l_p = 21.28 μm. Interestingly, the persistent length estimated here and bending rigidity imposed in this study ($\kappa_b = 1.243\times10^{-17}$ N m) satisfy the following well-known relation:

$$l_p = \frac{\kappa_b d}{k_B T} \tag{14}$$

where κ_b is multiplied by d for converting the unit of κ_b from [Nm] to [Nm^2]. In addition, the diffusivity of free actin monomers was also measured by calculating their mean square displacement (MSD). Fig. 2(a) shows an example of thermal fluctuation of a free monomer for 0.01 sec. By averaging such thermal trajectories, the smooth MSD curve was obtained as shown in Fig. 2(b). Using the Einstein diffusion equation, $< r^2 > \sim 6Dt$, the diffusivity of actin monomers, D, was estimated to be 7.5×10^{-8} cm^2/s that falls within the range of typical values of proteins in liquids [10]. Through these validations, it was confirmed that the model simulating Brownian dynamics and semiflexible polymer works correctly.

Fig. 3(a) shows an instance of the distribution of filament length, L_f, with $P_n = 10^{-7}$. The distribution

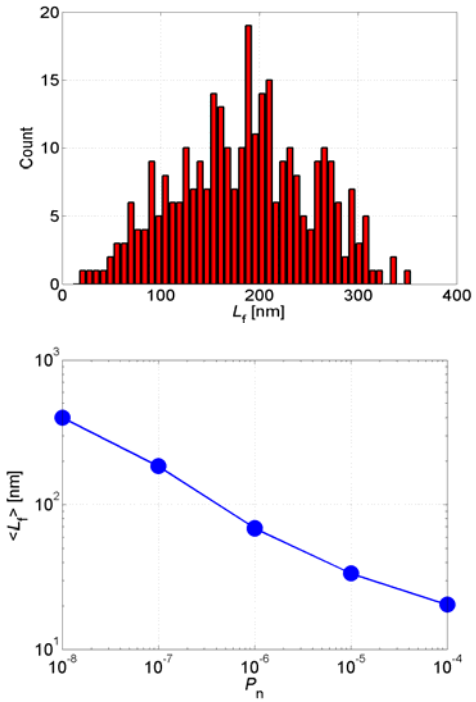

FIG 3. (a) An example of filament length distribution similar to normal distribution, where P_n is 10^{-7}. The mean filament length, $<L_f>$, is 184 nm. (b) Average of filament length distribution at different P_n. The mean value tends to be inversely proportional to P_n.

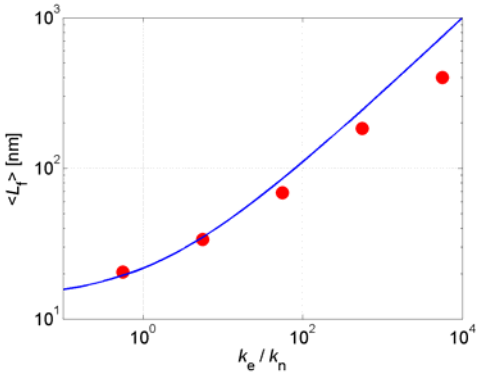

FIG. 4. Average filament length depending on k_e / k_n obtained from the continuum approach (blue line) and computational model (red circles). They show a remarkable agreement with a small amount of deviation at large k_e / k_n.

appears to be somewhat analogous to normal distribution with $<L_f>$ = 184 nm and also to one of the experimental results [11]. In Fig. 3(b), as can easily be guessed by one's intuition, the average filament length is inversely proportional to P_n. As described before, this simulation model has only a minimal set for actin polymerization and thus should have several artifacts. For example, in reality, the elongation rate on a filament is not constant but dependent on the status of the free monomer (ATP or ADP) and also on the age of the filament [4]. Furthermore, a number of actin binding proteins that highly affect polymerization process *in vivo* can lead to the totally different length distribution of actin filaments. However, the result shown here is meaningful in that it can provide insight into relations between polymerization process and fundamental rates.

We can compare the average filament length obtained using the computational model with theoretical predictions. First, the values of k_n and k_e are obtained by Eqs. (7) and (8), and the average filament length is plotted with theoretical values (Eq. (12)). In Fig. 4, results from two dissimilar methodologies exhibit a quite nice agreement at a wide range of k_e / k_n while there is a small deviation between the two that grows as k_e / k_n increases. The large k_e / k_n corresponds to a case with long filaments, so the deviation might have been caused since in the case, a pool of free actin monomers can be quickly depleted near the barbed end of a filament. If the depletion of the pool occurs, it takes time for the barbed end to encounter available free monomers diffusing closely to it. During the delay, more nucleation events can happen, resulting in a larger number of filaments with shorter length. Despite the small deviation, the correspondence between two results is quite remarkable considering the very different nature of the methods.

In this study, the length distribution of actin filaments was investigated using the computational model and the continuum approach. The overall distribution is similar to normal distribution with a mean value inversely proportional to the nucleation probability, P_n. In comparison of the result acquired using the computational model with that obtained via the continuum approach, they exhibited a nice agreement despite the different nature of the two methodologies. There are a number of possible applications which can be performed as the extension of this study. For example, we can estimate the effect of depolymerization on length distribution. In addition, several actin binding proteins such as gelsolin capping proteins can be implemented here via either explicit or implicit method, and their influences can be probed.

[1] J. Howard, *Mechanics of Motor Proteins and the Cytoskeleton* (Sinauer Associates, Sunderland, 2001).
[2] H. Lodish, et al., *Molecular Cell Biology*. 5th ed. (W. H. Freeman and Company, New York , 2004).
[3] D. Sept and J.A. McCammon, Biophys. J. **81**(2), 667-674 (2001).
[4] T.D. Pollard, J. Cell Biol. **103**(6), 2747-2754 (1986).
[5] P.T. Underhill and P.S. Doyle, J. Non-Newton. Fluid **122**(1-3), 3-31 (2004).
[6] D.C. Rapaport, *The Art of Molecular Dynamics Simulation* (Cambridge University Press, New York, 1995).
[7] H. Higuchi, T. Yanagida, and Y.E. Goldman, Biophys. J. **69**(3), 1000-1010 (1995).
[8] H. Isambert, et al., J. Biol. Chem. **270**(19), 11437-11444 (1995).
[9] D.M. Marini, *Structure and Formation of β-Sheet Fibers*, in *Mechanical Engineering* (Massachusetts Institute of Technology, Cambridge, 2003).
[10] G.A. Truskey, F. Yuan, and D.F. Katz, *Transport Phenomena in Biological Systems*, 2nd ed. (Prentice Hall, New York, 2008).
[11] D. Biron and E. Moses, Biophys. J. **86**(5), 3284-3290 (2004).